STRAIGHT-LINE TRACK RECONSTRUCTION IN 3D IMAGES USING ADAPTIVE MORPHOLOGICAL HOUGH TRANSFORM

Aline R. Gesualdi	José M. Seixas	Márcio P. Albuquerque
Electrical Engineering Department	Signal Processing Laboratory	Coordination of Technical Activities
CEFET/RJ	LPS/COPPE/UFRJ	CBPF
Av. Maracanã, 229	Centro de Tecnologia, H220	Rua Dr. Xavier Sigaud, 150, 3o andar
Rio de Janeiro, RJ, Brazil	Cidade Universitária	Rio de Janeiro, RJ, Brazil
email: agesualdi@cefet-rj.br	Rio de Janeiro, RJ, Brazil	email: albuquer@cbpf.br
	email: seixas@lps.ufrj.br	

ABSTRACT

In the paper, a hybrid image processing approach – the adaptive morphological Hough transform AMHT – is developed and applied to detect straight line tracks in the volumetrical images produced by particle collisions in the ATLAS detector. The approach combines components of the adaptive Hough transform (i.e. the resolution refinement of the parameter space) and the morphological Hough transform (i.e. using a morphological mask to increase the chance for detecting the correct peak in Hough space). Experimental results show that the new AMHT method improves the detection efficiency from 86% to 89% while maintaining the timing requirements.

KEY WORDS

Hough Transform, Adaptive Hough Transform, Morphological Mask, Track Reconstruction, ATLAS Detector

1. Introduction

The Hough Transform (HT) is a feature extraction technique proposed by Hough in 1962 [1]. Up to now, hundreds of papers have been published on the issues related to HT. These issues include a lot of applications, variants, and extensions of HT. Illingworth and Kittler introduced the Adaptive Hough Transform (AHT) in 1987[2], which uses recursion in parameter space to increase detection peak efficiency, as well as, precision. Schmidt, Schimmler and Schröder in 1997 introduced the concepts of Morphological Hough Transform[3]. Their proposition convolves a morphological mask with parameter space, reducing noise and increasing peak detection.

Hough Transform parameter space can have, depending on its generation, a n to 1 point relation regarding to data space. Therefore, improvements to data space point selection mechanisms were also the goal of many studies throughout the years. In order to reduce HT computational timing only relevant points or pixels should be used to form the parameter space. For example, the Local Hough Transform (LHT) approach reduces parameter space complexity in straight line detection by peaking up pairs of pixels in data space to represent one point in parameter space[4].

Besides pair formation, resolution and noise reduction of parameter space are important to be studied, in order to increase efficiency and accuracy. The AHT varies the resolution of parameter space until a particular condition is satisfied. This condition is problem dependent and can be dynamically adjusted[5, 6]. By doing this, parameter space can be represented by small matrices, decreasing computational timing. In Schmidt implementation, the MHT convolves a morphological mask in parameter space in order to accomplish noise reduction. By doing this, spurious points in parameter space are eliminated, reducing noise, also the mask shape and size is problem dependent.

The concepts of HT in its adaptive, local and morphological form were specifically adjusted to a collision vertex detection problem, in high-energy physics. All images in this paper represent fragments of proton-proton collision simulations of the next-generation collider experiment, LHC (Large Hadron Collider). The collision point is obtained by detecting straight-lines in these volumetrical images, and has to meet an execution latency requirement of 1 ms. Because of these constraints, a detailed study of point relevance were made, as well as a study of noise reduction in parameter space.

The paper is organized as follows: Section 2 describes the AMHT; Section 3 details how 3D or volumetrical images are formed inside ATLAS detector; Section 4 shows how AMHT was used in vertex collision reconstruction; Section 5 presents the results obtained and; finally, Section 6 has the summary of our main conclusions.

2. The AMHT mechanism and its advantage

The AMHT consists of a hybrid implementation of AHT and MHT. Initially the system has no knowledge of target location. For this reason, a coarse granularity of the parameter space is defined. Resolution refinement of the parameter space occurs in subsequent iterations, as in AHT. The stopping condition consists of outlining a desired precision and, at each iteration, verifies if such condition was satisfied.

The adaptive mechanism reduces considerably the computational effort of HT. However, when adjacent bins
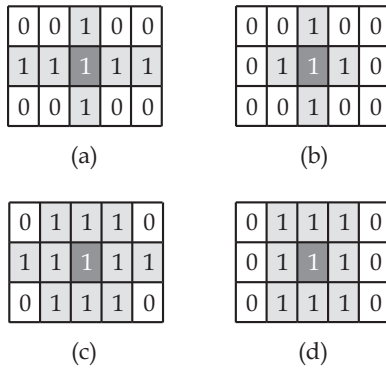
0	0	1	0	0
1	1	1	1	1
0	0	1	0	0

(a)

0	0	1	0	0
0	1	1	1	0
0	0	1	0	0

(b)

0	1	1	1	0
1	1	1	1	1
0	1	1	1	0

(c)

0	1	1	1	0
0	1	1	1	0
0	1	1	1	0

(d)

Figure 1. AMHT masks example.

in parameter space achieve similar heights at a coarse granularity, the adaptive method may choose the wrong bin to expand in the next loop, causing an error at the final iteration. This is corrected by using morphological masks. Not only is the maximum peak that is expanded to the next iteration, but all coincident bins within the morphological mask marked as 1. The size and shape of the mask may vary according to the problem. We tested four different masks in our system, as depicted in Figure 1. Detection efficiency was measured to each of the four masks, where good eficiency is set when a distance less than 1 mm is found between the detected line and the desired one. Mask 1(c) had the best efficiency result. By doing this test with different masks, we noticed the relevance of mask shape and size in detection efficiency.

An interesting point to address out is the fact that, in this case of straight-line track detection, the mask is not convolved in the parameter space, at variance from Schmidt implementation. First, the maximum bin is detected, then the mask center is positioned on this bin. With the mask at this position, each parameter space bin is multiplied by the correspondent mask bin, resulting at another parameter space. Figure 2 presents the block diagram of the AMHT.

The main advantage of using AMHT is that it is more precise than AHT and LHT, once the shape of mask represents parameter space characteristics. A restriction of this method is computational timing and the determination of best structuring element.

3. 3D Image Formation in ATLAS Detector

First this section describes the ATLAS detector, giving priority to track reconstruction constraints. In the sequence, it explains how the 3D images are formed. At the end, an example of a volumetrical image is presented.

3.1 ATLAS Detector

The ATLAS (A Toroidal LHC ApparatuS) detector[8] is one of the multi-purpose detectors currently under construction at the Large Hadron Collider (LHC). Its inner
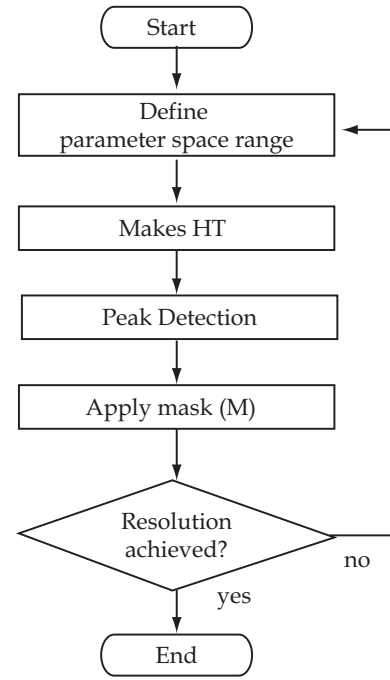
Figure 2. AMHT block diagram.

elements are tracking detectors enclosed in a solenoidal magnet of around 2T in the central part. From the inside to the outside, it consists of pixel detectors, silicon strip detectors (SCT) and transition radiation detectors (TRT). The tracking detectors are surrounded by a electro-magnetic calorimeter based on liquid Argon technology and a hadronic calorimeter. The global detector dimensions are defined by a large air-core muon spectrometer[9].

The ATLAS trigger system must accept the high 40MHz bunch crossing frequency and reduce it to a manageable rate of roughly 200 Hz. It is comprised of a three-level system. The first-level hardware-based trigger (Level-1) quickly analyzes data from the calorimeter and muon spectrometer systems to derive an accept or reject decision within 2 μs. Events are passed on to a second-level software-based trigger (Level-2) at a rate of 75 kHz which must derive a decision within an average latency of 10 ms. Level-2 accepted events are passed on to the third-level software-based Event Filter (EF) at a rate of roughly 3 kHz which has a more generous latency of roughly 1 s to pass the event on to offline mass storage with a rate of roughly 200 Hz. It is axiomatic that only events surviving this three-stage triggering system can be part of subsequent physics analysis. Together, the Level-2 and EF are referred to as the High Level Trigger (HLT)[10].

The online track reconstruction occurs at the HLT. Primary vertex reconstruction represents the first of four stages of the track reconstruction chain[11]. The position of collision vertex in ATLAS is expected to vary within ± 15 cm around the center of the detector ($z = 0$) along the beam direction, or z direction. A precise knowledge (≤ 1
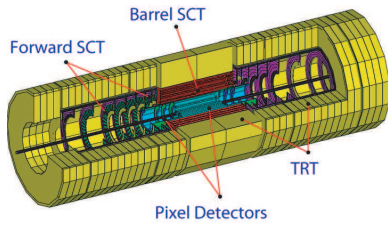
Figure 3. Three-dimensional view of ATLAS Inner Detectors.

Figure 4. An example of a volumetrical image. This is a single-e shown by Pixel and SCT detectors. (a) $\rho \times z$ e (b) $\phi \times z$.

mm) of the z-position (z_{vtx}) is of high interest, once it can improve performance and reduce execution time for pattern recognition in ATLAS tracking detectors[12].

In this paper we describe an algorithm which evaluates z_{vtx} using 3D or volumetrical images from ATLAS tracking detectors Pixel and SCT (Semiconductor Tracker). The algorithm is based on the quasi-linear relationship between track trajectories in a uniform magnetic field. Therefore, the helix equation that governs tracks is approximated to a line equation[12]. The target of HT is to detect the z origin of $\rho = mz + b$ equation, where m is the line slope and b is the ρ interception.

3.2   Illustrating the Events

A three-dimensional cutaway view of the layout of the Inner Detector is shown in Figure 3. The Pixel detector is designed to provide a very high-granularity, high-precision set of measurements as close to the interaction point as possible[13].

The SCT system is designed to provide four precision measurements per track in the intermediate radial range, contributing to the measurement of momentum, impact parameter and vertex position, as well as providing good pattern recognition by the use of high granularity[13].

The volumetrical image is composed only by the detector areas sensibilized by particles. Therefore, the 3D image is a chained list of space points in cylindrical coordinate (SP(ϕ, ρ, z)). Figure 4 presents an example of a volumetrical image. It shows the p-p collision product as a single electron (single-e).

The HT algorithms were evaluated over $\approx$10,000 single-e events or volumetrical images. These events were divided in two sets: development and testing sets. The collision point to be found by HT is a simulation target, i.e., already known. Therefore, a collision vertex found by HT was considered as correct if it was less than 1 mm far away from the simulation target.

4. Collision vertex reconstruction using AMHT

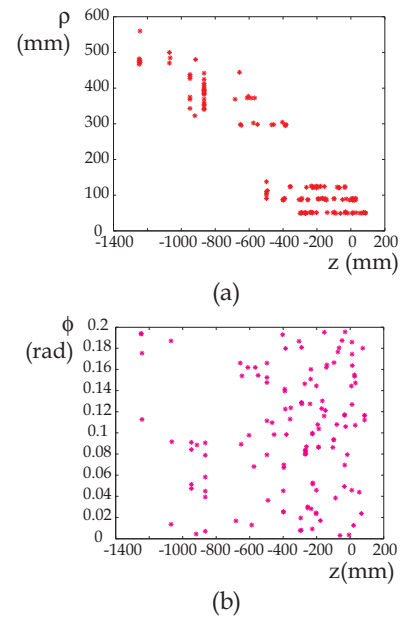The vertex reconstruction system was divided in two blocks: Space Point Selection and Collision Vertex Detec-

tion. The Space Point Selection had two purposes. The first one was to reduce the computational effort for the next step, *i.e.*, the Collision Vertex Detection. The second was to improve system efficiency.

The Collision Vertex Detection block performs fully localization of the primary vertex by means of HT. This block receives on its input the filtered space points of the Space Point Selection block. Three variations of Hough transform were tested. The first one consists on the Local Hough Transform, second is the Adaptive Hough Transform and third is the Adaptive Morphological Hough Transform.

4.1   Space Point Selection

The space point selection method establishes a distance where space points can interact, called contour area. The contour area ray is determined in $\phi \times z$ direction. Only space points inside this area will be used by Hough Transform.

Another space point selection restriction is on how points inside the contour area are to be combined. Space points within the same ρ value, i.e., belonging to the same detector barrel were not combined. By doing this, the noise caused by indiscriminate combination of points was avoided.

The output of this block is a chained list of filtered space points, SP(ϕ, ρ, z). This list is the input of Collision Vertex Detection block.

4.2 Collision Vertex Detection

The HT algorithms were implemented in this block. A total of three different methods of Hough Transform were tested for comparison, which are:

- Local Hough Transform (LHT)

    The Local Hough Transform, as described in Dantas[14] was implemented. All pair combination of space points from the chained list provided by Space Point Selection Block were used to form Hough's' parameter space.

    The parameter space matrix had a fixed number of bins for all single-e events. The development set of events were used to determine the parameter space range.

- Adaptive Hough Transform (AHT)

    The Adaptive Hough Transform, as described in Illingworth[2], was implemented. All pair combinations of space points from the chained list provided by Space Point Selection Block were used to form Hough's' parameter space.

    The parameter space matrix varies in accordance with events. A fix number of recursions were used. The development set of events determined the initial parameters for AHT, which are: 4 number of recursions and the parameter space input range for all events.

- Adaptive Morphological Hough Transform (AMHT)

    The AMHT method described in Section 2 was implemented. As above, all pair combinations of space points from the chained list provided by Space Point Selection Block were used to form Hough's' parameter space.

    As in AHT, the parameter space varies accordingly to the event. Four recursions were also determined by the development set of events. The morphological masks used are depicted on Figure 1. Figure 1(a) had the best efficiency under development set, thus being chosen for final system design, which was evaluated from the testing set.

5. Results

Results were obtained using simulated data of single-e in high luminosity with pile-up[15]. The maximum computation timing allowed for vertex detection was 1 ms scaled to a 4 GHz machine.

    The image database was divided in two sets: development and testing, each one with ≈5000 samples. The
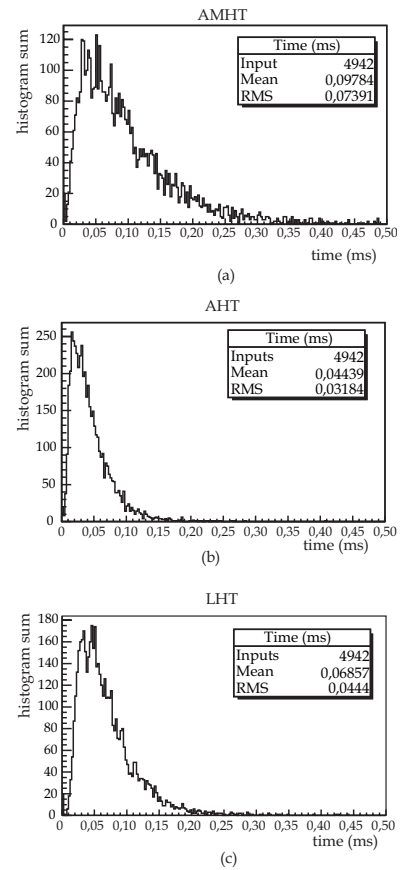

Figure 5. Computation timing measurements of testing samples for (a) AMHT implementation; (b) AHT and (c) LHT.

samples used in development set were to adjust the algorithm parameters in order to improve efficiency. The testing set was used to verify system efficiency. The results are presented over testing samples.

    Table 1 presents results obtained by AMHT, AHT and LHT. All values presented in this table are the mean and standard deviation, in brackets, of computational timing in milliseconds. The table is organized as follows: the first column displays the HT algorithm, the second column indicates the average timing of the Space Point Selection filter; the third column contains the HT average effort; the next column is the average of the total time and; the last column is the efficiency, i.e., vertexes within a range of 1 mm from the true one.

    As we can observe from Table 1 the hybrid implementation of Hough Transform (AMHT), had the best efficiency and a good timing result, i.e., less than 1 ms. One aspect relevant to point out is that all results were measured on the same machine and using the same testing set. Therefore a straightforward comparison can be made. The computation timing histogram for all HT implementations can be depicted in Figure 5.

    The computation timing was measured with respect to the number of space points at the input of AMHT and

HT algorithm	t_{SP}(ms)	t_{HT}(ms)	t_{total}(ms)	Ef ciency
AMHT	0.0704($\pm$ 0.0093)	0.0266($\pm$ 0.0219)	0.0978($\pm$ 0.0739)	4403/4942(89.09%)
AHT	0.0702($\pm$ 0.0093)	0.0271($\pm$ 0.0232)	0.0959($\pm$ 0.0316)	4260/4942(86.19%)
LHT	0.0712($\pm$ 0.0093)	0.0342($\pm$ 0.0228)	0.1065($\pm$ 0.0424)	3652/4942(73.89%)

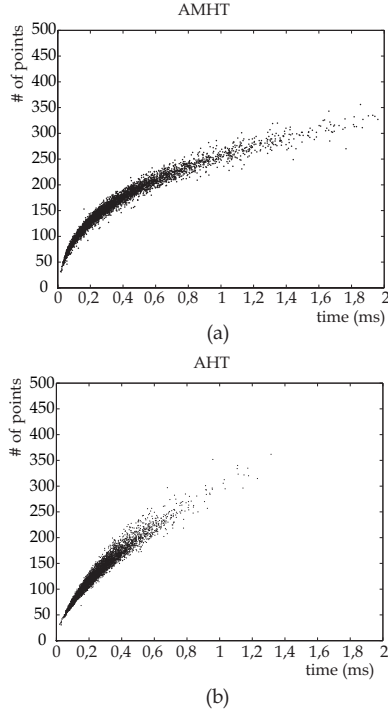Table 1. Results from different HT algorithms. See text.

Figure 6. Computational timing of (a) AMHT and (b) AHT in relation to the number of space points at HT input.

Figure 7. Vertex Difference Histogram, i.e., difference of simulated vertex (z_{true}) and calculated by (a) AMHT and (b) AHT (z_{vtx}).

AHT, as shown in Figure 6. There is an exponential relation between computational effort and the number of points for both HT implementations.

Figure 7 shows the difference between true collision vertexes (z_{true}) and calculated by AMHT and AHT algorithms (z_{vtx}). This figure shows how accurate and precise are those methods. For AMHT $\approx$89% of the events were inside the 1 mm difference range and the other 11% are very close to this range. Almost the same characteristic was observed for AHT, where $\approx$86% of events were inside the 1 mm difference range and the ones not inside this range are very close.

6. Conclusion

This paper presented a hybrid version of Hough Transform, where adaptive and morphological flavors were combined. Approximately ten thousand samples were used to adjust and verify HT efficiencies. Computation timing measurem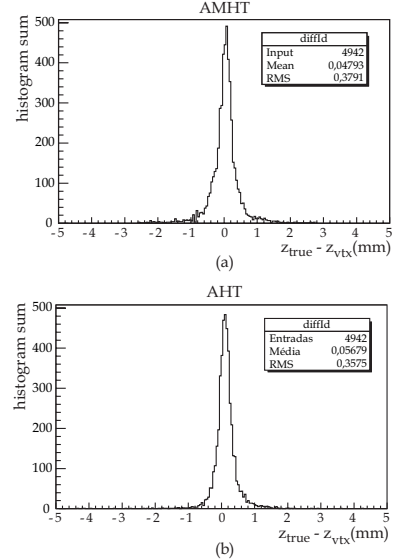ents were also a figure of merit, once the collision vertex determination had speed constraints in ATLAS online trigger chain.

Three different implementations of Hough transform were evaluated. As observed in Section 5 AMHT had the best collision vertex detection and accomplished the timing constraints.

All tests made with testing samples were implemented in the actual ATLAS Trigger system, called The ATHENA[16]. The hybrid AMHT is in agreement with ATLAS restrictions, showing to be a good tool for collision vertex reconstruction.

The advantage of AMHT method is that it combines the speed of the Adaptive Hough Transform with the morphological characteristics of parameter space. The AMHT achieved and effciency of 89% in vertex collision reconstruction, within an average timing performance of 0.09 ms per collision event.

Acknowledgement

References

[1] HOUGH P.V.C.; Method and Means for Recognizing Complex Patterns; *U.S. Patent 3069654*, Dec. 18, 1962.

[2] ILLINGWORTH J.; KITTLER J.; The adaptive Hough transform; *IEEE Trans. Pattern Anal. Mach. Intell.*, vol. 9, issue 5, 1997, ISSN: 0162-8828, pp 690–698, IEEE Computer Society, Washington, DC, USA.

[3] SCHMIDT B.; SCHIMMLER M.; SCHRÖDER H.; Morphological hough transform on the instruction systolic array; *International Euro-Par conference No3*, Passau , Germany, vol. 1300, 1997, ISBN 3-540-63440-1, pp. 798–806.

[4] DANTAS A.C.H., SEIXAS J.M., FRANÇA F.M.G., Parallel Implementation of a Track Recognition System Using Hough Transform; *VECPAR*, 2000, pp 467–480.

[5] GURU D.S.; SHEKAR B. H.; NAGABHUSHAN P., A simple and robust line detection algorithm based on small eigenvalue analysis, *Pattern Recogn. Lett.*, vol. 25, issue 1, 2004, ISSN: 0167-8655, pp. 1–13, http://dx.doi.org/10.1016/j.patrec.2003.08.007, Elsevier Science Inc., New York, NY, USA.

[6] YANG S.M, et al; Weld line detection and process control for welding automation, *Meas. Sci. Technol.*, vol. 18, 2007, pp. 819-826, doi:10.1088/0957-0233/18/3/034, IOP Electronic Journals.

[7] SIM L.C.; SCHRODER H.; LEEDHAM G.; Major line removal morphological hough transform on a hybrid system, *J. Parallel Distrib. Comput.*, vol. 64, issue 9, 2004, ISSN: 0743-7315, pp. 1060–1068, http://dx.doi.org/10.1016/j.jpdc.2004.05.006, Academic Press, Inc., Orlando, FL, USA.

[8] ATLAS Collaboration, ATLAS: Technical Proposal for a General-Purpose pp Experiment at the LHC, *CERN/LHCC/94-43*, 1994.

[9] GESUALDI, A. R. ; SEIXAS, J.M.; BAINES, J. T. M. ; ELSING, M. ; ANJOS, A. ; BEE, C. P. ; PADILLA, C. ; WIELERS, M.; ARMSTRONG, S. ; GEORGE, S. . Overview of the High-Level Trigger Electron and Photon Selection for the ATLAS Experiment at the LHC. *IEEE Transactions on Nuclear Science*, v. 53, p. 2839-2843, 2006.

[10] ARMSTRONG, S. ; GESUALDI, A. R. ; SEIXAS, J. M. ; ELLIS, N. ; GROUP, Altas Tdaq . Algorithms for the ATLAS High Level Trigger. *IEEE Transactions on Nuclear Science*, v. 51, p. 367-374, 2004.

[11] SCHIAVI C.; CERVETTO M.; PARODI F.; KONSTANTINIDIS N.; SUTTON M.; BAINES J.; EMILUIYANOV D.; DREVERMANN H.; Fast tracking for the second level trigger of the ATLAS experiment using silicon detectors data; *Nuclear Science Symposium Conference Record*, 2004 IEEE, vol. 3, pp. 1841-1844, ISSN: 1082-3654, ISBN: 0-7803-8700-7, INSPEC Accession Number: 8650940, Digital Object Identi er (DOI): 10.1109/NSSMIC.2004.1462602.

[12] KONSTANTINIDIS N.; DREVERMANN H.; Determination of the z position of primary interactions in ATLAS, *ATLAS Press*, Geneva, CERN, 16 Jul 2002, 7 p, ATLAS Notes: ATL-SOFT-2002-007.

[13] DITTUS F.; HAYWOOD S.; Inner Detector Technical Design Report, *Atlas Notes*, ATLAS TDR 4, CERN/LHCC/97-16, ISBN: 92-9083-102-2, 1997.

[14] FRANÇA, F. ; SEIXAS, J. M.; DANTAS, A. C. H. . Parallel Implementation of a Track Recognition Systrem Using Hough Transform. *Lecture Notes in Computer Science*, Germany, pp. 467-480, 2001.

[15] ATLAS Collaboration Detector and Physics Performance; *Technical Design Report*, Volume I, CERN/LHCC, 1999.

[16] BROKLOVÁ Z.; Simulations of ATLAS silicon strip detector modules in ATHENA framework; *DSc. Thesis; Institute of Particle and Nuclear Physics*, Prague, August 2004.